



Influence of impurity and recycling on high- β steady-state plasmas sustained by rotating magnetic fields current drive

H.Y. Guo*, J.A. Grossnickle, A.L. Hoffman, G.C. Vlases

University of Washington, Redmond Plasma Physics Laboratory, 14700 NE 95th Street, Suite 100, Redmond, WA 98052, USA

ARTICLE INFO

PACS:
52.25.Vy
52.40.Hf
52.30.-q
52.50.Gj
52.55.Hc

ABSTRACT

A new upgrade of the Translation, Confinement, and Sustainment (TCS) device, TCSU, has been built to form and sustain high temperature compact toroids (CT), known as Field Reversed Configurations, using Rotating Magnetic Fields (RMF). In TCS the plasma temperature was limited to several 10s of eV due to high impurity content. These impurities are greatly reduced in TCSU by using advanced plasma chamber and helium glow discharge cleaning. Reducing impurity radiation, when coupled with reduced overall recycling, enabled the plasma to enter into a new, collisionless regime with temperatures well over 200 eV, substantially exceeding the radiation barrier. This is a first for CTs at low input power density. This was achieved using the simple even-parity RMF drive (despite transient opening of field lines by the RMF) because the associated energy loss is sheath-limited, coupled with the low edge density resulting from the RMF pinch effect.

© 2009 Elsevier B.V. All rights reserved.

1. Introduction

A field-reversed configuration (FRC) [1] is a subclass of compact toroids (CT), which have singly connected magnetic geometry without toroidal field coils and center column. Moreover, FRCs have zero, or very small self-generated toroidal fields and consequently very high β (ratio of plasma to magnetic pressure, approaching 100%), coupled with a natural, linear, unrestricted magnetic divertor, thus offering an unusual potential for an economic fusion reactor. In addition, it can be used for disruption mitigation and fuelling for other types of magnetic fusion reactors. It also offers an attractive option for advanced space propulsion, and is relevant to astrophysical jets and coronal mass ejections.

FRCs have been produced by various techniques such as field-reversed θ -pinch, coaxial slow source [2], and merging spheromaks with opposite helicities [3]. The Translation, Confinement, and Sustainment (TCS) device demonstrated the formation and steady-state sustainment of FRCs over 50 normal flux decay times, using rotating magnetic fields (RMF) [4], which also provided complete FRC stability [5]. However, in TCS the plasma was radiation dominated with the temperature limited to several 10s of eV due to high impurity content. A new TCS-upgrade device (TCSU) [6] has now been built with a bakeable, ultra-high vacuum chamber, and advanced wall conditioning capabilities. Impurities are greatly reduced in TCSU, allowing much higher temperatures for a given

RMF field and input power. The higher temperature achieved in TCSU, coupled with reduced global hydrogenic recycling, enabled the plasma to enter into a new high-confinement, collisionless FRC state with a dramatic improvement in current drive. The present paper, which reports on these advances, is organized as follows. The most basic aspects of the FRC formation and sustainment using RMF are described in Section 2, where effects of plasma flow for driving current throughout are also discussed. A rough estimation of impurity content in TCSU from impurity doping experiments is presented in Section 3, where comparisons of radiative losses are also made between TCS and TCSU. Overall properties of the newly achieved high temperature FRCs in TCSU are presented in Section 4. Power losses due to open field line convection are examined in Section 5 using a one-dimensional, sheath-limited, model. Finally, a summary and conclusions are given in Section 6.

2. Principle of FRC formation and sustainment using RMF

Fig. 1 illustrates the most basic aspects of the RMF current drive process. The rotating magnetic fields are generated by driving the currents in the vertical and horizontal antennas 90° out of phase. The RMF frequency ω must be higher than the ion cyclotron frequency $\omega_{ci} = eB_\omega/m_i$, where B_ω is the RMF vacuum field, but much lower than the electron cyclotron frequency $\omega_{ce} = eB_\omega/m_e$, i.e., $\omega_{ci} < \omega \ll \omega_{ce}$, in order for electrons, but not ions, to follow RMF rotation. The RMF torque on the electrons is equal to [7]

$$T_{\text{RMF}} = (2\pi r_s^2 B_\omega^2 / \mu_0) \ell_a f(\zeta), \quad (1)$$

* Corresponding author. Address: P.O. Box 7010, Rancho Santa Margarita, CA 92688, USA.

E-mail address: hguo@trialphaenergy.com (H.Y. Guo).

where r_s is the separatrix radius, B_{ω} the RMF vacuum field, and ℓ_a is the RMF antenna length. $f(\zeta)$ is a function of the ratio of average electron rotation frequency to RMF frequency, $\zeta \equiv \langle \omega_e \rangle / \omega = \frac{2B_e/\mu_0}{\frac{1}{2}(n_e)e\omega r_s^2}$, where B_e is the maximum sustained poloidal field. To generate the poloidal magnetic flux, the applied RMF torque T_{RMF} must exceed the resistive torque due to electron-ion collisions,

$$T_{\eta} = \frac{1}{2} \pi e^2 (n_e^2 \omega_e \eta_{\perp}) r_s^4 \ell_s, \quad (2)$$

where η_{\perp} is the cross-field resistivity and ℓ_s is the FRC length. The poloidal flux changes according to:

$$\frac{d\phi_p}{dt} = \frac{2}{n_e e r_s^2 \ell_s} (T_{RMF} - T_{\eta}). \quad (3)$$

In steady-state, the applied RMF torque is balanced by the resistive torque, and the ratio of the maximum possible sustained poloidal magnetic field to the applied RMF vacuum field,

$$\frac{B_e}{B_{\omega}} \propto \sqrt{\frac{\omega r_s^2 \zeta}{\eta_{\perp}}}. \quad (4)$$

Since the RMF usually does not fully penetrate the FRC, typically only to the magnetic axis, $R = r_s/\sqrt{2}$, an inward flow has to be driven to sustain the current on the inner field lines. This can be seen by a simple Ohm's law

$$E_{\theta} = \eta_{\perp} j_{\theta} + \langle -\tilde{v}_{ez} \tilde{B}_r \rangle + v_r B_z - v_z B_r. \quad (5)$$

The bracketed term is the RMF drive force due to oscillating axial electron motion in phase with the radial part of the RMF. On the outer flux surfaces this must be strong enough to not only overcome the negative resistive term, but also drive an inward radial flow to sustain the current on the inner field lines (where the axial field B_z is negative), thus allowing E_{θ} to be uniformly zero. It has been observed that the FRC can be sustained far beyond the RMF antenna. Outside the antenna at the ends, again the RMF drive is not available, and thus the current must be maintained by the steady axial flow, coupled with the B_r field, which is naturally present at the FRC ends.

3. Impurity content in TCSU

A schematic of the TCSU facility is shown in Fig. 2. TCSU is a highly-modified version of TCS with an entirely new translation and confinement section, which is bakeable and built to ultra-high vacuum (UHV) specifications with integral glow discharge cleaning (GDC) system and provisions for titanium gettering and siliconiza-

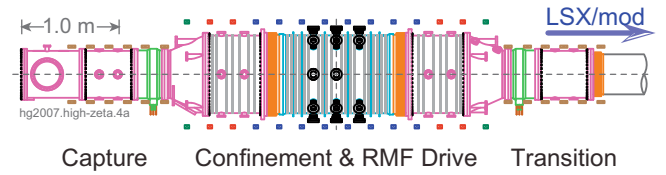


Fig. 2. Schematic of TCSU device.

tion wall conditioning. As in TCS, FRCs can be produced either by rotating magnetic fields, or by expanding and translating high- β energetic plasmoids formed by the LSX (Large s Experiment)/mod θ -pinch into the confinement and RMF drive chamber.

As expected, impurity radiation is greatly reduced in TCSU by using a bakeable, ultra-high vacuum chamber and routine helium (He) glow discharge cleaning (GDC). Fig. 3 compares the total radiation measured by the bolometer between TCSU and TCS under similar RMF operating conditions. As can be seen, the FRCs in TCS were clearly radiation dominated. In contrast, the FRCs in TCSU exhibit much lower radiative losses, with a radiation fraction, $P_{rad}/P_{in} \sim 1/3$. He GDC also reduces global recycling levels, greatly facilitating density control.

To estimate impurity content in TCSU, we carried out a series of experiments where our usual operating gas, deuterium, was doped with small percentages of impurity gas, so that the background plasma conditions are not significantly affected. In this case, the intrinsic impurity content can be estimated by comparing the changes in the impurity line radiations with and without doping.

The experiments were performed using a standard operating condition (in 100% D_2 fill gas). The gasses used for doping were CD_4 , CO_2 , SiH_4 , N_2O , and N_2 , and the atomic impurity concentration ranged from $\sim 0.25\%$ to upwards of 4% for most fill gasses. SiH_4 was limited to $\sim 0.125\%$ to $\sim 0.5\%$ range due to the danger of high concentrations of Silane in our vacuum system. During the experiments we had 3 monochromators set to monitor C III, O III, and Si III. We were also able to monitor a N III line that was very near the Si III line. In addition, we were able to use a multi-channel ICCD spectrometer to get some axial resolution as well as to monitor other impurities and confirm our monochromator measurements.

Analysis of the data shows that during the steady-state period the concentration of silicon is approximately 0.3%, oxygen is approximately 3%, and carbon is inferred to be approximately 0.5% from both CD_4 and CO_2 doping. The N_2O doping experiments did not yield useful results due to drastic performance degradation with introduction of more than 0.1% atomic nitrogen (confirmed by N_2 doping).

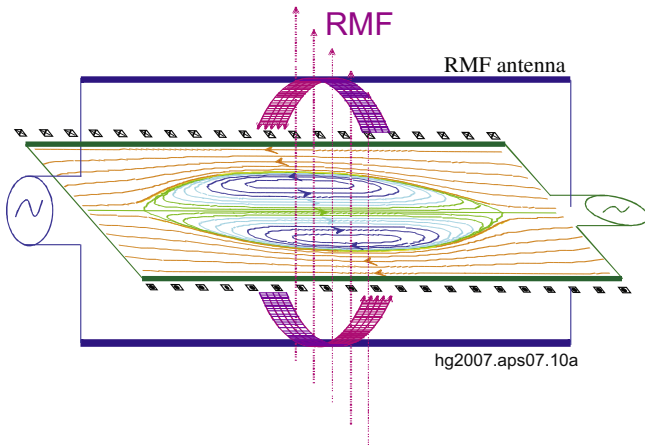


Fig. 1. Illustration of RMF current drive process for an FRC.

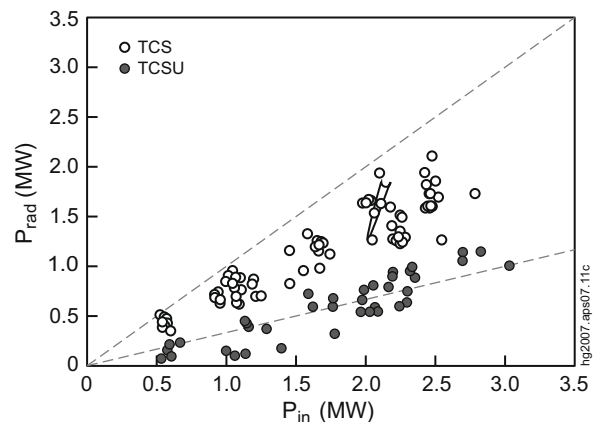


Fig. 3. Comparison of radiative losses between TCS and TCSU.

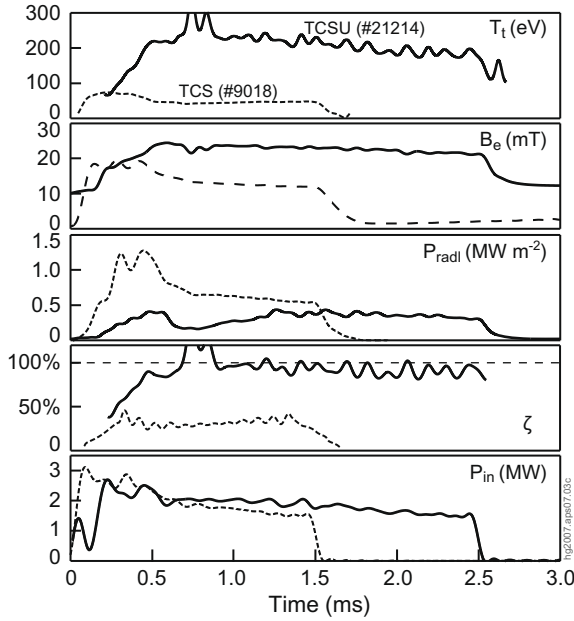


Fig. 4. Time traces for two FRCs formed in TCS and TCSU with the same RMF field strengths and similar frequencies: 114 kHz for TCS, and 117 kHz for TCSU.

4. Global behavior of high temperature FRCs in TCSU

Fig. 4 shows the global properties of two comparable FRCs achieved in TCSU and TCS. Both discharges have similar RMF field strength, B_ω , and similar RMF frequencies with $f = \omega / (2\pi) = 117$ kHz for TCSU, and 114 kHz for TCS. As can be seen, the radiated power P_{rad} is significantly reduced in TCSU, compared to TCS. Consequently, the total temperature ($T_t = T_i + T_e$) shows more than a five-fold increase in TCSU. T_i is derived from radial pressure balance accounting for the RMF B_θ contribution, i.e., $p \approx (B_e^2 + \frac{1}{2}B_\theta^2) / 2\mu_0 = n_m k T_t$, with $B_\theta = 2B_\omega$ and $n_m = \langle n_e \rangle / \beta$. It is truly remarkable that ζ , a measure of current drive efficiency, approaches and stays close to unity throughout the entire discharge. Consequently, much higher poloidal field, B_e , is sustained in TCSU, as predicted by Eq. (4).

Such a high- ζ FRC state exhibits the following key features [8]: (1) dramatic improvement in current drive efficiency with ζ approaching 100% for the first time in TCSU; (2) up to three-fold increase in global energy confinement time; and (3) significant reduction in transport rates, accompanied by a striking transition from a Bohm-like transport to a LHD-like transport. For a given mass, the LHD-type transport rates, $D_{LHD} \propto \rho_*^{-2} D_{Bohm}$, where $\rho_* = \rho_i / r_s$ is the normalized ion Larmor radius. This scaling is even better than gyro-Bohm, $D_{gB} \propto \rho_* D_{Bohm}$, and as such is very favorable for next step FRC development.

5. Convective power losses

As shown by detailed measurements from a triple Langmuir probe in TCS [9], the electron temperature of the RMF formed and sustained FRCs exhibits a nearly flat radial profile throughout. However, the particles are well confined with the density at the separatrix, n_s , only about 0.2 n_m , where n_m is the peak density. This is, at least in part, attributed to the intrinsic inward flow driven by the RMF, as described in Section 2. The density falls rapidly outside the separatrix in the scrape-off layer (SOL) with a decay length, $\lambda_n \sim 0.02$ m.

Parallel energy transport along the field lines in the SOL is largely determined by classical conduction and convection. Due to

short connection length, $L_c \sim \frac{1}{2} \ell_{FRC}$, i.e., the half length of the FRC, the SOL plasma for an FRC is usually in the so-called ‘sheath-limited’ regime [10], which is characterized as

$$v_\sigma^* \equiv L_c / \lambda_\sigma < 10, \quad \sigma \in e, i, \quad (6)$$

where λ_σ is the Coulomb collision mean free path with $\lambda(m) = \lambda_i \sim \lambda_e \approx 2 \times 10^{15} T_i(\text{eV})^2 / n_e(\text{m}^{-3})$ for $T_i = T_e$. In this regime, the open field line plasma is essentially isothermal along \mathbf{B} , the energy losses are convective, and thermal conduction is small. Thus, energy loss is governed by the heat transmission properties of the sheath at the boundary, i.e., the divertor target plates, i.e.,

$$q_{sh} = \frac{1}{4} n_s C_s k T_t \gamma_{sh}, \quad (7)$$

where the ion sound speed $C_s = \sqrt{k T_t / m_i}$, and the sheath heat transmission factor, $\gamma_{sh} \sim 8$, includes both ion and electron contributions. Thus, the total power loss, due to convective energy flow along field lines to divertors at both ends, is

$$P_{conv} = 2 \int q_{sh} 2\pi r dr \approx 4\pi r_s \lambda_n q_{sh}. \quad (8)$$

Taking into account radial pressure balance, i.e., $n_m k T_t \approx B_e^2 / 2\mu_0$, the loss power can be expressed as

$$P_{conv} = \frac{\pi r_s \lambda_n \gamma_{sh} B_e^2}{2\mu_0} \sqrt{\frac{k T_t}{m_i} \left(\frac{n_s}{n_m} \right)}. \quad (9)$$

Fig. 5 plots the calculated convective loss power, P_{conv} , as a function of total input power from RMF, P_{in} , for typical FRCs in TCS and TCSU. As can be seen, P_{conv} approaches $\sim 50\%$ P_{in} , in TCSU, significantly higher than in TCS. Thus, it is essential to minimize power loss through field line opening by using odd-parity RMF current drive [11,12] for further improvement in FRC performance.

6. Summary

Improvements in the vacuum quality and glow discharge cleaning in TCSU have led to great reductions in impurity content. Dedicated impurity doping experiments with CO_2 , CD_4 and SiH_4 showed that oxygen is the dominant impurity present in TCSU, $\sim 3\%$. Reduced impurity radiation, coupled with reduced recycling losses result in dramatic increases in temperature, from 10s of eV to well over 200 eV, and significant improvement in current drive efficiency with ζ approaching 100%. This was achieved using the simple even-parity RMF drive, despite instantaneous opening of field lines by the RMF. This is because the associated energy loss is sheath-limited, coupled with the low edge density resulting

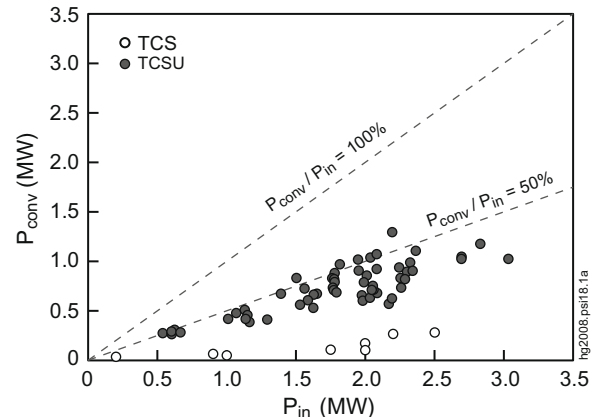


Fig. 5. Convective power losses estimated from a simple sheath-limited model for typical plasma conditions in TCS and TCSU.

from the RMF pinch effect. Further improvements may be achieved by advanced wall conditioning such as Ti gettering to minimize impurity radiation, and using odd-parity RMF current drive to reduce open field line losses.

Acknowledgements

The authors wish to acknowledge support from the rest of RPPL team. This work was supported by the US Department of Energy.

References

- [1] M. Tuszewski, Nucl. Fus. 28 (1988) 2033.
- [2] Z.A. Pietrzyk et al., Nucl. Fus. 27 (1987) 1478.
- [3] Y. Ono et al., Phys. Rev. Lett. 76 (1996) 3328.
- [4] A.L. Hoffman, H.Y. Guo, K.E. Miller, R.D. Milroy, Nucl. Fus. 45 (2005) 176.
- [5] H.Y. Guo, A.L. Hoffman, R.D. Milroy, et al., Phys. Rev. Lett. 94 (2005) 185001.
- [6] K.E. Miller, J.A. Grossnickle, R.D. Brooks, et al., Fus. Sci. Technol. 54 (2008) 946.
- [7] H.Y. Guo, A.L. Hoffman, R.D. Milroy, Phys. Plasmas 14 (2007) 112502.
- [8] H.Y. Guo, A.L. Hoffman, R.D. Milroy, et al., Phys. Plasmas 15 (2008) 056101.
- [9] S.P. Andreason, J.T. Slough, Bull. Am. Phys. Soc. 48 (2003) 146.
- [10] P.C. Stangeby, The Plasma Boundary of Magnetic Fusion Devices, IOP, Bristol, 2000.
- [11] S.A. Cohen, R.D. Milroy, Phys. Plasmas 7 (2000) 2539.
- [12] H.Y. Guo, A.L. Hoffman, L.C. Steinhauer, Phys. Plasmas 12 (2005) 062507.